Original Article

Role of Exosomes from Mesenchymal Stem Cell in Hepatic Regeneration After Acute Liver Damage by Carbon Tetrachloride in Adult Male Albino Rats (Histological Study)

Ghada Lotfy, Nevert Farid Abd El Salam, Seham Kamel Abounasef and Samar F. Ezzat

Department of Histology, Faculty of Medicine, Ain Shams University, Egypt

ABSTRACT

Introduction: Acute liver failure (ALF) is one of the emergency illnesses Bone marrow mesenchymal stem cell derived (BM-MSC) exosomes are broadly used in recovering medicine.

Aim of the Work: Demonstration of the role of BM-MSC exosomes in hepatic regeneration after acute liver damage induced by carbon tetrachloride model in adult male albino rats.

Materials and Methods: 55 adult male albino rats were separated into three groups: Group I (control), group II [given a single intraperitoneal injection (0.05 ml/kg) of carbon tetrachloride (CCl4) and group III [given a single tail vein injection of 50 µg of BM-MSC exosomes in 100 µl phosphate buffered saline 24 hours post-CCl4]. The rats were sacrificed after 7 and 14 days. Histological examination of liver tissue was performed with biochemical analysis of AST and ALT.

Results: Group II revealed altered hepatic architecture with focal cellular access. Congestion and widening of portal and central veins. Sinusoids appeared disorganized and obliterated. Most hepatocytes had deeply acidophilic cytoplasm with condensed nuclei, while others were seen with pyknotic nuclei and vacuolation in cytoplasm. Collagen fibers were significantly increased. Examination by electron microscope showed hepatocytes with irregular heterochromatic nuclei and rarified cytoplasm with plenty of lipid droplets. Mitochondria decreased in numbers and sizes. Hepatic stellate cells were devoid of lipid droplets. Blood sinusoids showed multiple Kupffer cells. ALT & AST levels were significantly elevated. The exosomes treated rats showed improvement of the previously mentioned histological and biochemical changes.

Conclusion: Failure of liver regeneration and repair through 2 weeks after CCl4 induced toxicity. A single dose of bone marrow mesenchymal stem cells derived exosomes improved the hepatic regeneration after acute injury induced by CCl4.

Received: 12 August 2024, **Accepted:** 31August 2024

Key Words: Exosomes, hepatocytes, microscopic, rat, regeneration.

Corresponding Author: Samar F. Ezzat, MD, Department of Histology, Faculty of Medicine, Ain Shams University, Egypt, **Tel.** +2 010 0184 2765, **E-mail:** doc.rania@samarezzatali@yahoo.com

ISSN: 1110-0559, Vol. 47, No. 3

INTRODUCTION

Through the inactivation and effective removal of harmful chemicals and metabolites, the liver had a significant responsibility in biological detoxication of xenobiotics. The goal of metabolic processes involved in detoxications is to make xenobiotics more polar and water soluble[1]. The causes of acute liver failure (ALF) vary. When the amount of liver cells damage surpasses the capacity of hepatic regeneration, ALF becomes apparent. Worldwide, hepatitis caused by viruses and medications are the two most frequent causes of ALF[2]. Acute and extensive damage to the liver cells cause the abrupt loss of liver function. Death eventually follows additional deterioration into multiple organ failure, septicemia, and cerebral oedema[3].

Currently available treatments include plasma exchange, liver transplantation, non-natural liver treatment, and; however, there are limitations due to scarcity of livers of donor, the transient nature of artificial liver therapy, the high rate of post-operative complications, and the high financial expenditures[4]. Many researchers are interested in bone marrow MSC-exosomes as an innovative cell-free technique used in liver revival[5].

The International Society for Extracellular Vesicles (ISEV) defined Extracellular vesicles (EVs) as particles with lipid bilayer. They are emitted by cells spontaneously and lack the ability to replicate[6]. Exosomes are produced by late endosomes or multivesicular bodies (MVBs) budding as intraluminal vesicles (ILVs)[7]. Exosomes are recognized as drug carriers despite their innate biological activity because of their tiny size, excellent propensity to transfer beneficial components like proteins, nucleic acids, and tiny compounds[8].

It is now known that exosomes containing proteins, lipids, and nucleic acids peculiar to a particular cell can function as a channel for intercellular communication.

DOI: 10.21608/ejh.2024.309444.2117

Exosomes have the promise to interact with target cells, changing their behavior and phenotypic characteristics[9]. Exosomes of MSCs are widely used in regenerative medicine to treat a variation of disorders, contributing to the majority of MSCs' therapeutic benefits. Exosomes provide an opportunity for cell-free therapy, which lessens the concerns about employing live cells in a safe manner[10].

Ghasempour *et al*.[11] evidenced that MSCs secrete exosomes that are simpler, smaller, and less immunogenic than their parent cells. This helps to prevent the pulmonary embolism, iatrogenic tumor growth, and cell rejection load that come with transplanting MSCs, which is better than using correlated MSCs.

Since exosomes are recognized as transporters that lump many signal transduction pathways, much research was done to determine how exosomes and ALF interact and if they have the ability to chunk multiple signal transduction pathways to reduce fibrosis and inflammation in the liver and, consequently, the decline in organ failure[12].

Bala *et al*.[13] stated that carbon tetrachloride (CCl4) causes oxidative stress, apoptosis, and fibrosis in mice, it is frequently employed in ALI models. These effects are similar to those observed in the majority of liver illnesses in humans. So, goal of this research was to demonstrate the role of exosomes from mesenchymal stem cell on hepatic regeneration in acute liver damage caused by carbon tetrachloride in adult male albino rats histologically and biochemically..

MATERIALS AND METHODS

Cells

Isolation and culture of MSCs from young weaned male rat`s bone marrow was done at Stem Cell Research Unit, ASU, Faculty of Medicine, Department of Histology, based on Anastasio *et al*.[14]. The femurs and tibiae of the rats were dissected and immersed in 70% alcohol then transferred to centrifuge tubes containing PBS. In laminar flow hood, bones were washed in PBS solution three times, ends of the femurs and tibia were cut. Each bone shaft was flushed with 2 ml of complete culture media. The marrow plugs were collected and dissociated. The dispersed cells were centrifuged at 1400 round per minute (rpm) for 10 minutes in a Bench top centrifuge. The whole media was aspirated and added for suspension. Suspension of bone marrow cells in 10 ml of culture media in a T-75 flask. Incubation of the flasks was done at humidity (85%), 37°C, CO2 (5%). Before culturing, calculation of the cells and examination of their viability was done using the hemocytometer. Fifty microliters of the culture media containing the cells were mixed with trypan blue and were examined by the inverted microscope. cell number was counted in four small squares. The cells that did not take the trypan blue stain were considered viable. The total number was divided by four to obtain the average number of cells. It was then multiplied by the dilution factor and 10^4. The starting cell count was estimated by equation: dilution factor ×Standard number of cells per small square $\times 10^4$. Aspiration of the culture media containing the non-adherent cells was done, while adherent cells were cleaned with a sterile phosphate buffer saline two times. When the cells became confluent, isolation of exosomes was done.

Isolation and Characterization of Exosomes

Isolation of exosomes was done by ultracentrifugation method according to Coughlan *et al*[15]. Ultracentrifugation was done at National Research Center, Cairo, Egypt by ultracentrifuge machine (Sorval-MTx150, made in Jaban). Resuspension of isolated exosomes in PBS (50–200 µl) was done for downstream use and were stored at -80°C. Characterization of exosomes[16] was done using transmission electron microscope (TEM), JEOL- 1010; 80kv, at Al- Azhar University in the Regional Center of Mycology and Biotechnology (RCMB), (Figure 1).

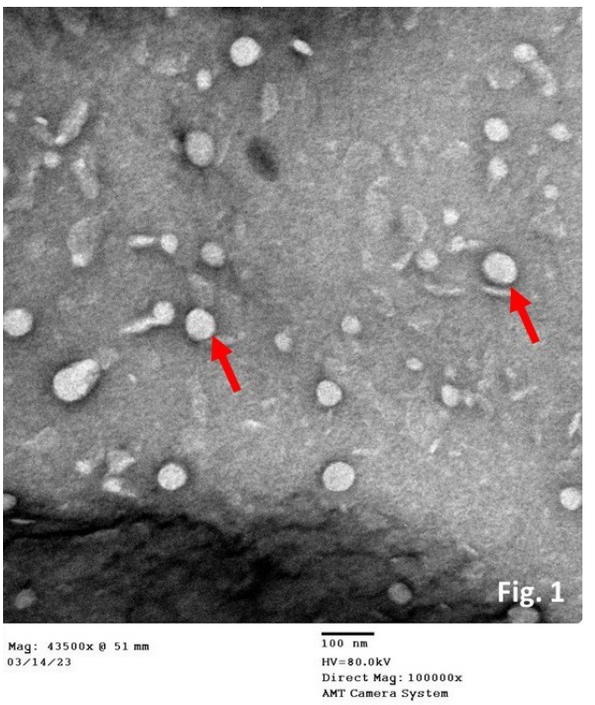

Fig. 1: Identification of MSC-Ex (↑) with transmission electron micrograph. Scale bar 100 nm

Animal Studies

The experiment took place at ASU, Faculty of Medicine, Medical Research Center. The scientific research ethical committee of the ASU Faculty of Medicine and animal care requirements were followed in carrying out all of the experimental procedures under Wide Assurance No. FWA000017585. Fifty-five adult male albino rats with average weight between 220–250 g was separated into three groups. Group I (Control group) (n=15) was then subdivided into Subgroup Ia was left without interference (n=5), Subgroup Ib was injected by olive oil buffer intraperitoneally (n=5) and Subgroup Ic was injected by phosphate buffered saline through tail vein (n=5). Group II

(CCL4 group) (n=20) were given a single intraperitoneal injection of (3% vol/vol in olive oil) at 0.05 ml/kg of carbon tetrachloride (CCl4). Group II was subdivided to subgroup IIa which was sacrificed after one week of CCl4 injection, and subgroup IIb which was sacrificed after two weeks. Group III (CCl4 + exosomes treated group) (n=20) were given 50 µg of exosomes in 100 µl phosphate buffered saline through tail vein 24 hours post-CCl4 for the treatment group. Group III was subdivided to subgroup IIIa which was sacrificed after one week of exosomes injection, and subgroup IIIb which is sacrificed after two weeks.

Biochemical and Histological Analyses

To measure aspartate aminotransferase (AST) and alanine aminotransferase (ALT), blood samples were taken from retro-orbital veins. All groups' right liver lobes were removed, fixed in 10% neutral buffered formalin, and then processed to create paraffin blocks. Haematoxylin and Eosin stain and Modified Masson's Trichrome staining were applied to five µm-thick slices[17]. Brief segments of liver tissue were quickly preserved by submerging them in 2.5% glutaraldehyde, and subsequently subjected to transmission electron microscopy (TEM) analysis[17]. The samples were inspected and captured on camera using a Japanese-manufactured JEOL-1010 TEM at the electron microscopy unit of the Al-Azhar University's Regional Centre of Mycology and Biotechnology (Cairo, Egypt).

Morphometry and Statistics

All the groups underwent morphometric analysis to determine the area % of collagen fibers. For morphometric research, a computer in the Department of Histology, Faculty of Medicine, ASU, was equipped with an image analyzer Leica Q win V.3 application. The Leica DM2500 microscope (Wetzlar, Germany) was linked to the computer. Three separate slides with measurements of every subgroup that was acquired from every animal were used. For every slide that was used, five randomly chosen non-overlapping fields were looked at. The mean ± SD was used to express all measurements. The SPSS statistical program, version 21, was used to compare groups using a one-way analysis of variance test (ANOVA) (IBM Inc., Chicago, Illinois, USA). *P value*<0.05 was used to determine the data's significance; $p>0.05$ is non-significant, and $p< 0.001$ is highly significant.

RESULTS

% of deaths

During the experiment, there were four rats died in the CCl4-treated group with 20% mortality rate. In the other groups, no further deaths were registered.

Clinical observation

The rats of the control group were alert and active during the two weeks of the experiment. After the first week, the rats of the subgroup IIa showed decreased activity and alertness. While rats of subgroup IIIa seemed more active and alert than subgroup IIa. After the second week, the rats of subgroup IIb demonstrated severely restricted locomotor function. While the motor function of rats of subgroup IIIb was as same as control group.

Gross examination of the liver (Figure 2)

After two weeks of the experiment, livers of control group had normal consistency, size, texture, and color with intact lobes. Whereas livers of CCl4 -treated rats of subgroup IIb displayed firmer consistency, brittle texture, and paler color in comparison with those of control groups. With the administration of exosomes in the subgroup IIIb, the liver appeared darker in coloration than that of CCl4 -treated rats, and with comparable texture to that of control group.

Histological findings

sections stained with H&E

Hepatocytes in the control group's liver tissue exhibited branching and anastomosing cords. Hepatocyte cords extended outward from the central vein within each plate. The hepatocytes had a polyhedral appearance, with rounded vesicular nuclei and granular acidophilic cytoplasm. A few cells seemed to have two nuclei. Flat endothelial cells bordered the central vein. Hepatic sinusoids drained into the central vein by passing between the hepatocyte cords. The nuclei of the endothelial cells lining the hepatic sinusoids were flat. In the sinusoids, kupffer cells with spherical nuclei were seen (Figure 3A).

The hexagonal traditional lobule has one portal canal at each corner. The portal triads that encircled the portal canals were made of loose stromal connective tissue. Three basic structures were observed embedded in connective tissue: a thin-walled portal venule lined with flat endothelial cells; a thicker, smaller-diameter branch of the hepatic artery lined with flat endothelial cells; and a bile ductule lined with a single layer of cubical epithelial cells (Figure 3B). After one week of CCl4 injection, the liver of subgroup IIa revealed obvious focal alteration in the hepatic architecture. Some hepatic lobules showed features of centrilobular and periportal necrosis Most of the hepatic lobules showed variable forms of affection in which some of their hepatocytes nearby the central vein appeared swollen and vacuolated with darkly stained nuclei. Others seemed smaller, their nuclei compacted and their acidophilic cytoplasm heavily discolored. Also, there were apparent dilated and congested hepatic sinusoids, portal veins and central veins which showed obvious endothelial discontinuity. Periportal cellular infiltration was markedly apparent (Figures 3C,D).

In Subgroup IIIa (one week after exosome injection), A notable improvement was observed in certain lobules of the liver, where the hepatocyte cords were arranged in an organized manner around the central veins. The majority of hepatocytes had pale acidophilic cytoplasm and spherical, vesicular nuclei. Central veins and blood sinusoids were almost identical to those of the control group (Figure

3E). Nonetheless, there was still noticeable mild portal venous congestion with little periportal cellular infiltration (Figure 3F).

After two weeks, most of the hepatic lobules of subgroup IIb showed marked distortion of their architecture with extensive affection of most of hepatic lobules. Hepatic cords appeared disorganized with dilated congested blood sinusoids in between. Some sections showed hepatic lobules with loss of hepatic tissue and nearby hemorrhagic areas. Most of the lobules showed several patches of deeply acidophilic hepatocytes with condensed nuclei. Most of the central veins showed congestion with discontinuation of their lining endothelium. In between the hepatocytes, cells with spindle-shaped nuclei were seen (Figure 4A). The portal veins appeared to be dilated and congested in the majority of the portal locations. There appears to have been an increase in bile ductules. There was very little invasion of mononuclear cells. Few cells displayed vesicular nuclei, but the majority of the hepatocytes surrounding the portal area displayed profoundly acidophilic cytoplasm and condensed nuclei (Figure 4B).

While the liver tissue of rats of subgroup IIIb demonstrated a noticeable improvement in the liver tissue's structure. It seems to be similar to the control group's. Organized branching and anastomosing cords of hepatocytes radiating from the central veins with blood sinusoids in between were seen in the majority of the hepatic lobules. The majority of the hepatocytes had pale acidophilic cytoplasm and spherical, vesicular nuclei. Endothelium layers that were still intact lined the central veins. Kupffer cells and flat endothelial cells bordered the blood sinusoids (Figure 4C). The hepatic artery, portal vein, and bile ductule were visible in the portal regions, and there was no longer any congestion or mononuclear cellular infiltration (Figure 4D).

Sections stained with Masson trichrome

In the control group, a small number of green collagen fibers were seen between the hepatocyte cords, around the portal triad, and around the central vein (Figures 5A,B). Collagen fibre content was higher in Subgroup IIa than in the control group's (Figures 5C,D). On the other hand, grouping IIIa displayed less collagen fibers than subgroup IIa (Figures 5E,F). Further evidence of increased collagen deposition was found in subgroup IIb (Figures 5G,H), but subgroup IIIb showed further evidence of decreased collagen deposition, which was similar to control group (Figures 5I,J).

Electron microscopy analysis revealed that the hepatocytes in the control group had rounded, euchromatic nuclei that had nucleoli and were encircled by nuclear membranes connected to peripheral heterochromatin. Numerous mitochondria with distinct cristae and variable shapes and sizes, a rough endoplasmic reticulum, and rosettes of glycogen granules were visible in the cytoplasm. Short microvilli were protruded into the lumen of bile canaliculi between adjacent hepatocytes. The nearby junctional complexes were clearly seen (Figure 6A).

In some sections Kupffer cells were located in the lumen of sinusoids with several pseudopods and many lysosomes in their cytoplasm. Multiple lipid droplets were detected in the cytoplasm of hepatic stellate cells (also known as Ito cells, stellate fat storage cells), which had an oval nucleus (Figure 6B).

Following a week-long CCl4 injection, the liver of subgroup IIa revealed that certain hepatocytes had irregularly shrunken nuclei with increased peripheral heterochromatin, as well as rarified cytoplasm. The number of mitochondria shrank, and they had an electron-dense appearance with barely noticeable cristae. Glycogen rossets and the rough endoplasmic reticulum were hardly visible. The hepatic stellate cells appeared devoid of lipid droplets with spindle shaped nuclei and nearby collagen fibrils (Figure 6C). Congestion of the blood sinusoids was obvious with an apparent increase in Kupffer cell number (Figure 6D).

After one week of exosomes injection, the liver of subgroup IIIa showed that in comparison to the control group, a small number of hepatocytes had smaller nuclei and appeared to have more heterochromatin. Rough endoplasmic reticulum as well as the quantity and size of mitochondria appeared to be increasing. The majority of the mitochondria had recognizable cristae as compared to subgroup IIa. While the glycogen granules were hardly seen (Figure 6E). Kupffer cells appeared located in the lumen of sinusoids. In the perisinusoidal space, HSCs showed no signs of lipid droplets within their cytoplasm and nearby collagen strands were detected (Figure 6F).

After two weeks, most of the hepatocytes of the liver of subgroup IIb showed plenty of lipid droplets of variable sizes and well-defined edges, most of them appeared with low electron density, and others were electron dense. Most of the hepatocytic nuclei appeared shrunken with irregular nuclear membranes and increased heterochromatin. Cristae were shown to be disorganized or to completely vanish in mitochondria (a condition known as cristolysis). RER couldn’t be demonstrated. The glycogen granules were hardly seen. Additionally, rarefaction was visible in a few cytoplasmic regions (Figure 7A). In addition, some areas of the cytoplasm showed rarefaction. Hepatic sinusoids were congested. Kupffer cells apparently increased in number and appeared with kidney shaped nuclei and multiple cytoplasmic lysosomes. Neutrophil cells with multi-segmented nuclei were also demonstrated (Figure 7B).

In subgroup IIIb, compared to group IIb, the majority of the hepatocytes in the EM sections appeared to be devoid of lipid droplets, their nuclei were rounder and contained less heterochromatin. It was evident that the quantity and size of mitochondria had increased, and they had distinct cristae, rER and glycogen rosettes were demonestrated. The bile canaliculus was clearly seen with short microvilli in their lumen as well as apparently seen junctional complexes between the hepatocytes (Figure 7C). The lipid droplets

were still present in the hepatic stellate cells, which were almost identical to those in group I (Figure 7D).

Morphometric analysis of area % of collagen fibers

Comparing the area% of collagen fibers in subgroups IIa and IIb (P<0.05) to that of the control group (group I), there was a significant increase. In contrast, the area % of collagen fibers in subgroups IIIa and IIIb was considerably lower (P<0.05) than in rats treated with carbon tetrachloride. But between the exosomes groups and the control group, there was no significant change (P>0.05) (Table 1, Histogram 1).

Biochemical results

After one week, the carbon tetrachloride group (subgroup IIa) had significantly higher serum ALT and AST levels (P<0.05) than the control group (Group I). Rats who were given exosomes (subgroup IIIa) had considerably lower levels of ALT and AST than the group that was given carbon tetrachloride (P<0.05). The levels of serum ALT and AST did not differ significantly (P >0.05) between the exosomes group and the control group. Following a two-week period, the carbon tetrachloride group (subgroup IIb) exhibited significantly higher serum ALT and AST levels (P<0.001) in comparison to the control group (Group I). ALT and AST levels were substantially lower in rats that received exosomes (subgroup IIIb) than in rats that received carbon tetrachloride (subgroup IIb) (P<0.05). (Table 2, Histogram 2) show that there was no significant difference (P>0.05) in the serum ALT and AST levels between the exosomes group and the control group (Group I).

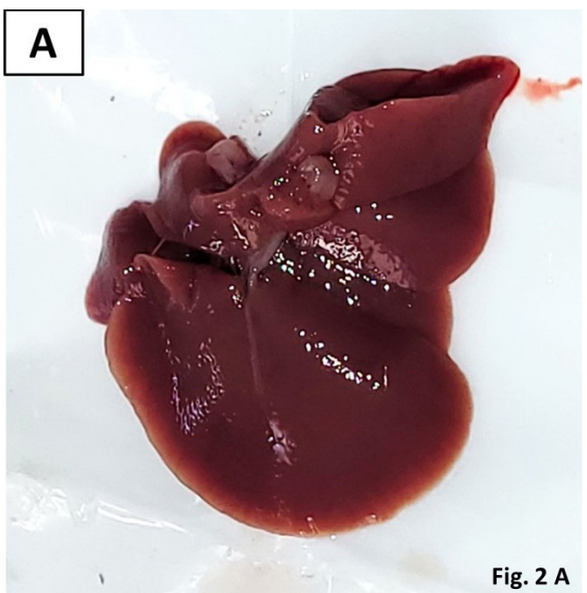

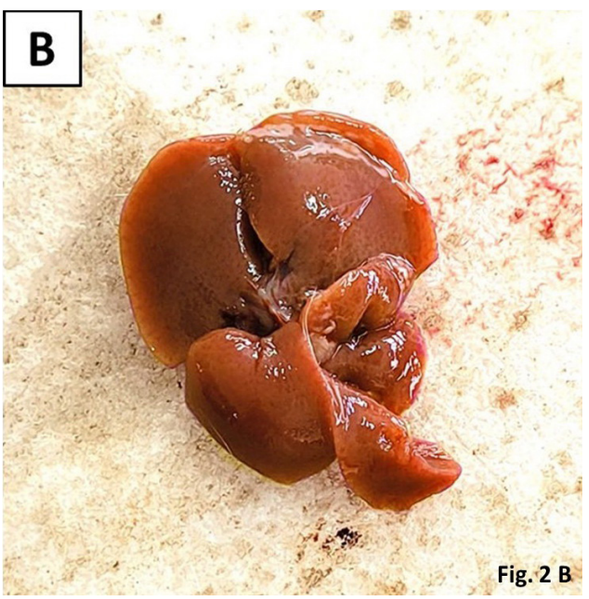

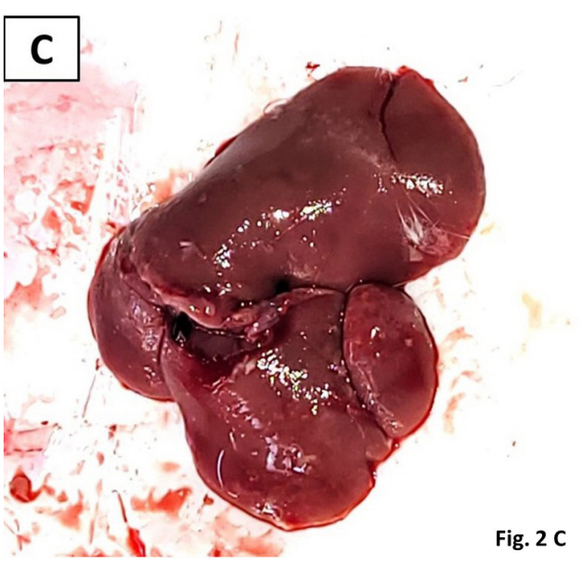

Fig. 2: The gross changes of the liver after treatment of induced acute injury by exosomes. A, control group shows normal reddish brown color with intact lobes. B, group IIb displays a pale light yellowish brown color and small size. C, group IIIb appears reddish brown.

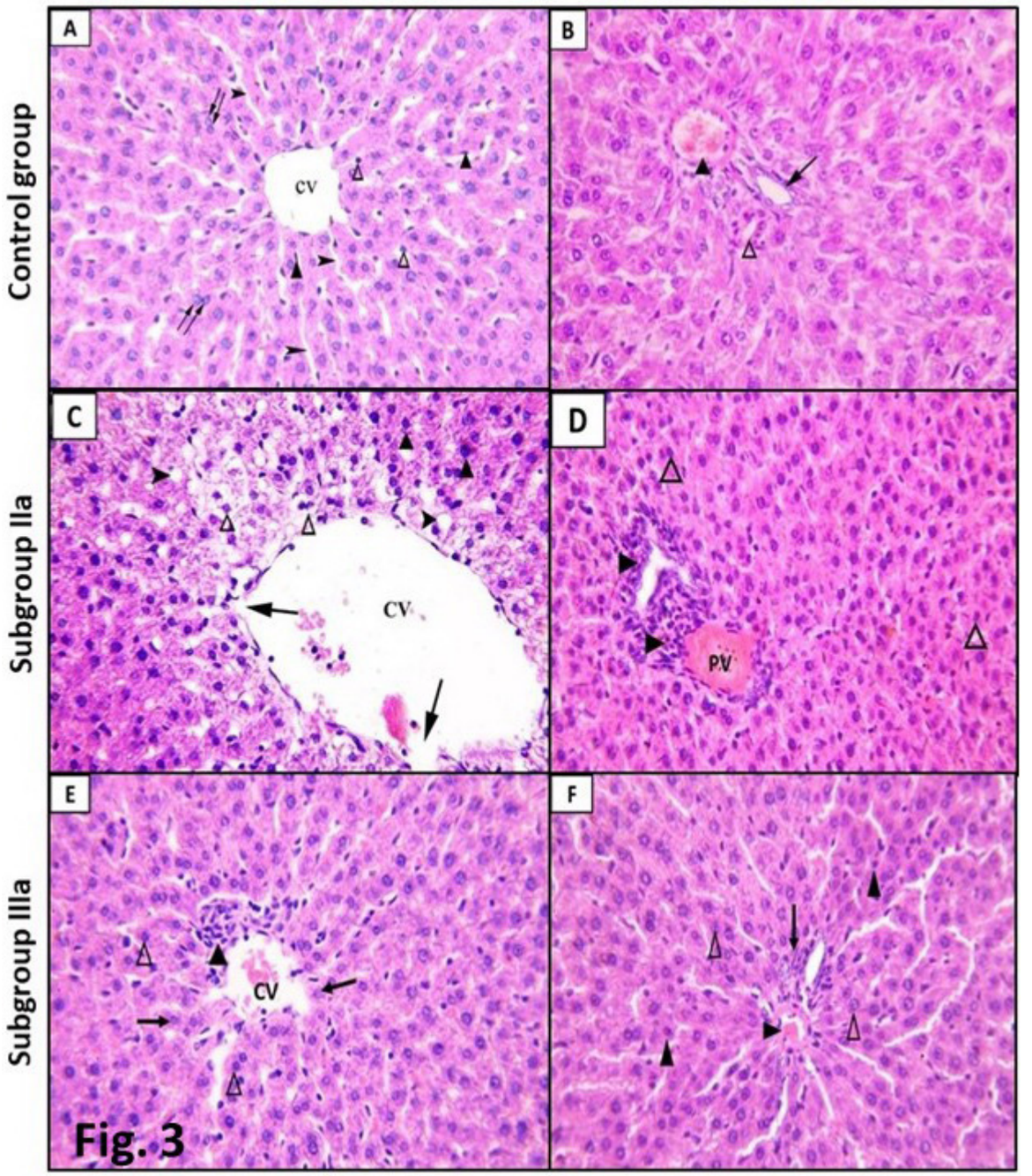

Fig. 3. H&E-stained sections of liver from different groups X400. [A, B]: control group, A, showing central vein (CV), hepatic cords with blood sinusoids (►) in between. Endothelial cells ▲and Kupffer cells Δ are lining the sinusoids. Binucleated cells (↑↑) are also seen. B, showing the portal triad, hepatic artery Δ, portal vein ▲ and bile ductule (↑). [C&D]: subgroup IIa, C, shows distorted hepatic architecture and obliteration of sinusoids (►). Dilated central vein (CV) with discontinuity of its endothelial lining (↑) is seen. Swelling and ballooning of some hepatocytes with vacuolated cytoplasm (Δ) in the centrilobular zone is noticed. Some hepatocytes appear with darkly acidophilic cytoplasm and condensed nuclei (▲). D, shows dilatation and congestion of portal vein (PV) with periportal cellular infiltration (►). Some hepatocytes appear with dark acidophilic cytoplasm and condensed nuclei (Δ). [E&F] subgroup IIIa, E, shows focal inflammatory cell infiltration (▲) near the central vein (CV). Most of the hepatocytes appear with vesicular central nuclei and pale acidophilic cytoplasm (↑). Few hepatocytes appear with condensed nuclei and dark acidophilic cytoplasm (Δ). F, shows the portal vein (►) with minimal periportal cellular infiltration (↑). Most of hepatocytes have pale acidophilic cytoplasm and vesicular nuclei (Δ), some few hepatocytes have condensed nuclei and dark acidophilic cytoplasm (▲).

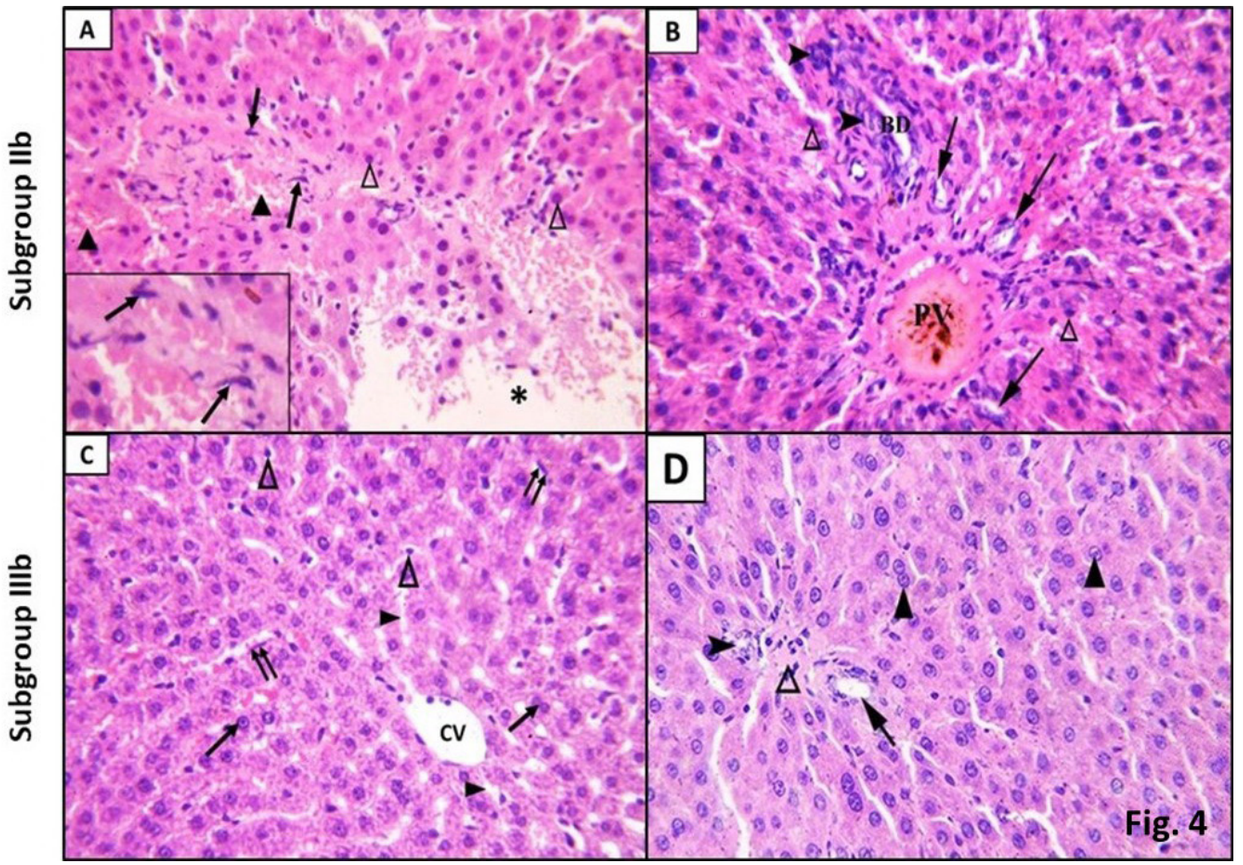

Fig. 4: H&E-stained sections of liver from different groups X400. [A&B]: subgroup IIb, A, shows marked distortion of hepatic architecture with loss of hepatic tissue (*) in some areas. Hepatocytes appear with condensed nuclei and dark acidophilic cytoplasm (Δ). The blood sinusoids are congested (▲). The inset shows cells with spindle shaped nuclei (↑) between the hepatocytes. B, shows dilatated congested portal vein (PV) with periportal cellular infiltration (►). Some hepatocytes have dark acidophilic cytoplasm and condensed nucleus (Δ). Notice the proliferation (↑) of the bile ductules (BD). Fig [C&D]: subgroup IIIb, C, shows branching and anastomosing cords of hepatocytes with rounded vesicular central nuclei and pale acidophilic cytoplasm (↑) around central vein (CV). Organized blood sinusoids (►) are seen between hepatic cords. Note the flat nuclei of the endothelial cells (↑↑) and the spherical nuclei of Kupffer cells (Δ) in the lining of the sinusoids. D, shows the portal vein (Δ), the hepatic artery (►), and a bile ductule (↑). Nearly all the hepatocytes (▲) in the periportal area display vesicular nuclei and pale acidophilic cytoplasm.

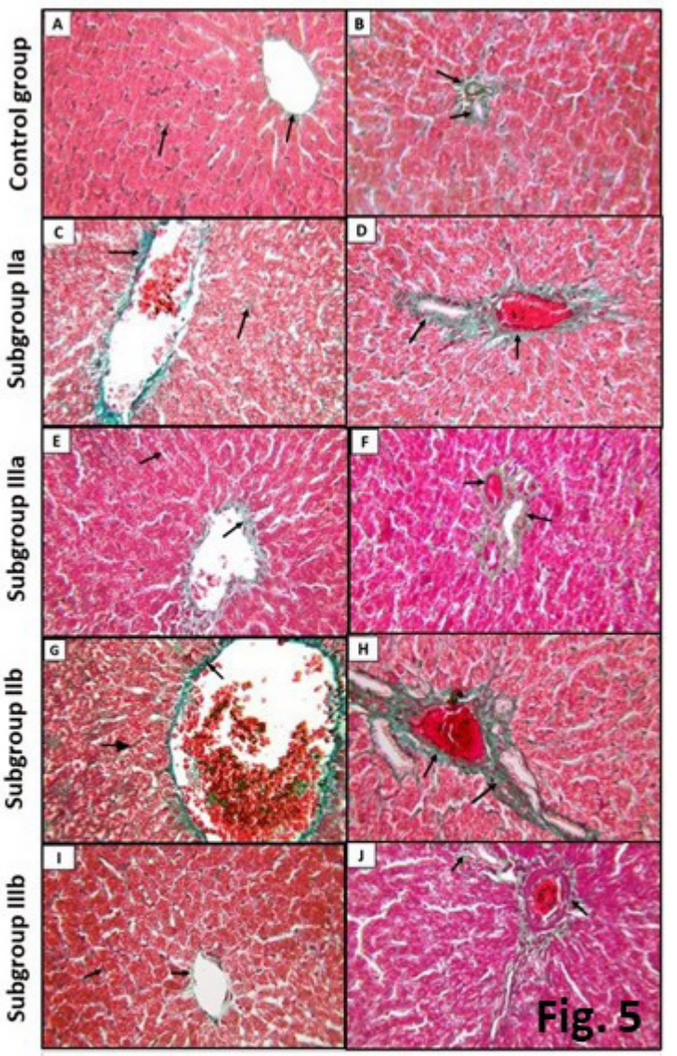

Fig. 5: Masson trichrome stained sections of liver from different groups X400. Green collagen fibers (↑) around central vein, portal vein, bile duct and between hepatic cords. [A&B] control group, [C&D] subgroup IIa, [E&F] subgroup IIIa, [G&H] subgroup IIb and [I&J] subgroup III.

Histogram (1) The mean values of area percentage of collagen fibers measured among the different groups.

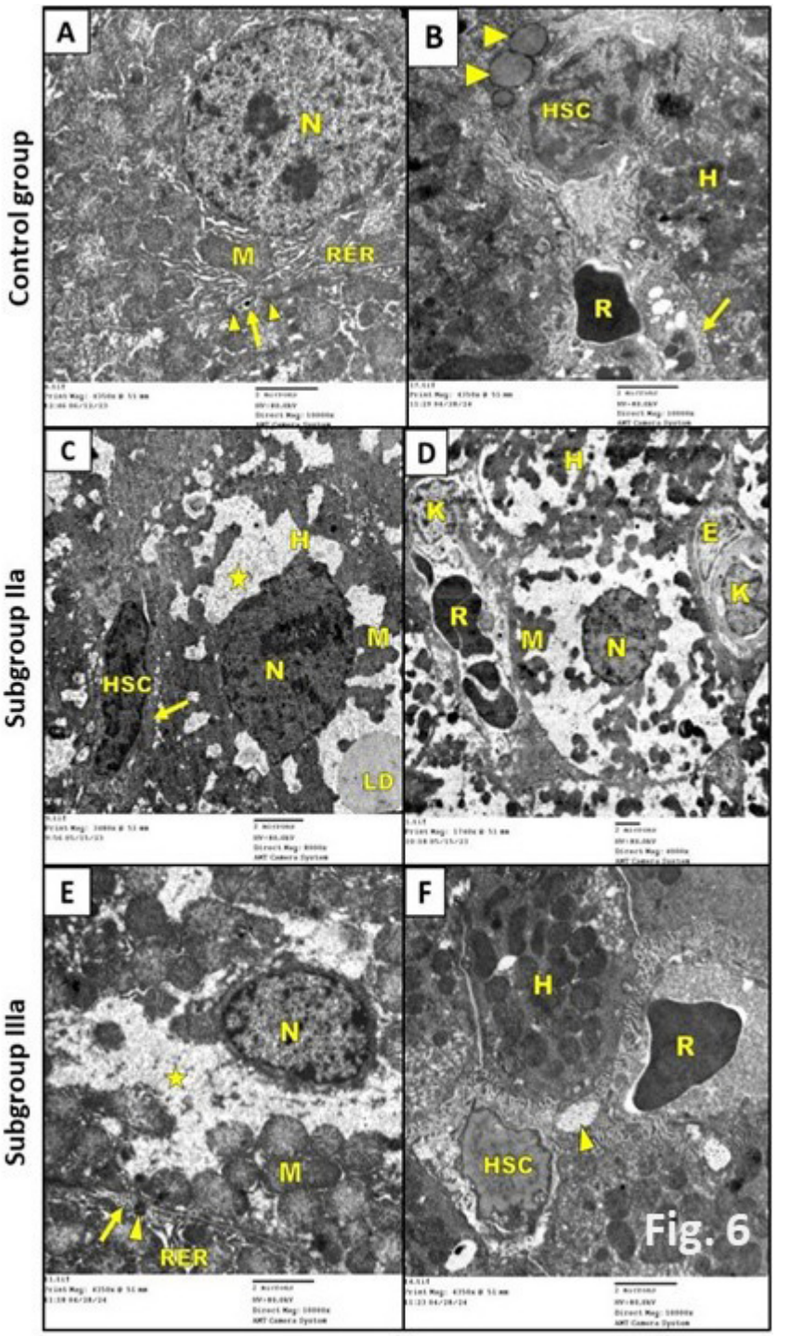

Fig. 6: transmission electron micrographs of different groups. [A&B] control group. A, shows euchromatic nucleus (N), multiple mitochondria of different size and shape with distinct cristae (M), and rough endoplasmic reticulum (RER). Notice the bile canaliculus in between adjacent hepatocytes (↑) and the nearby junction complex (▲). B, shows the blood sinusoids containing a red blood cell (R). Hepatic stellate cell (HSC) shows multiple lipid droplets in its cytoplasm (►). The perisinusoidal space contains the microvilli (↑) of the hepatocytes (H). [C&D]: subgroup IIa, C, shows heterochromatic nucleus (N) of the hepatocyte (H), few number of condensed coalesced mitochondria with indistinct cristae (M), a rarified cytoplasm (the star), and a lipid droplet in the cytoplasm (LD). Notice the spindle shaped nucleus of the hepatic stellate cell (HSC) with collagen fibrils nearby (↑). D, shows adjacent hepatocytes (H) separated by a cell membrane with heterochromatic nucleus (N), few number of condensed mitochondria with indistinct cristae (m), and a rarified cytoplasm. The blood sinusoid is full of RBCs (R). Notice the Kupffer cells (K) and the endothelial cell (E) in the lining of the sinusoids. [E&F]: subgroup IIIa. E, shows a nucleus (N) with increased peripheral heterochromatin, mitochondria with distinct cristae (M), RER profiles (RER), some areas of rarefaction (the star) in the cytoplasm. Notice the bile canaliculus in between adjacent hepatocytes (↑) with short microvilli projecting into its lumen, the nearby junction complex (▲) is also seen. F, shows hepatocytes (H) containing mitochondria with distinct cristae (M). The blood sinusoids contain a red blood cell (R), a hepatic stellate cell (HSC) devoid of lipid droplets in its cytoplasm with nearby collagen fibrils (▲) in the perisinusoidal space. TEM, Fig.A x10000, Fig.B x10000, Fig.C x8000, Fig.D x4000, Fig.E x10000, Fig.F x10000

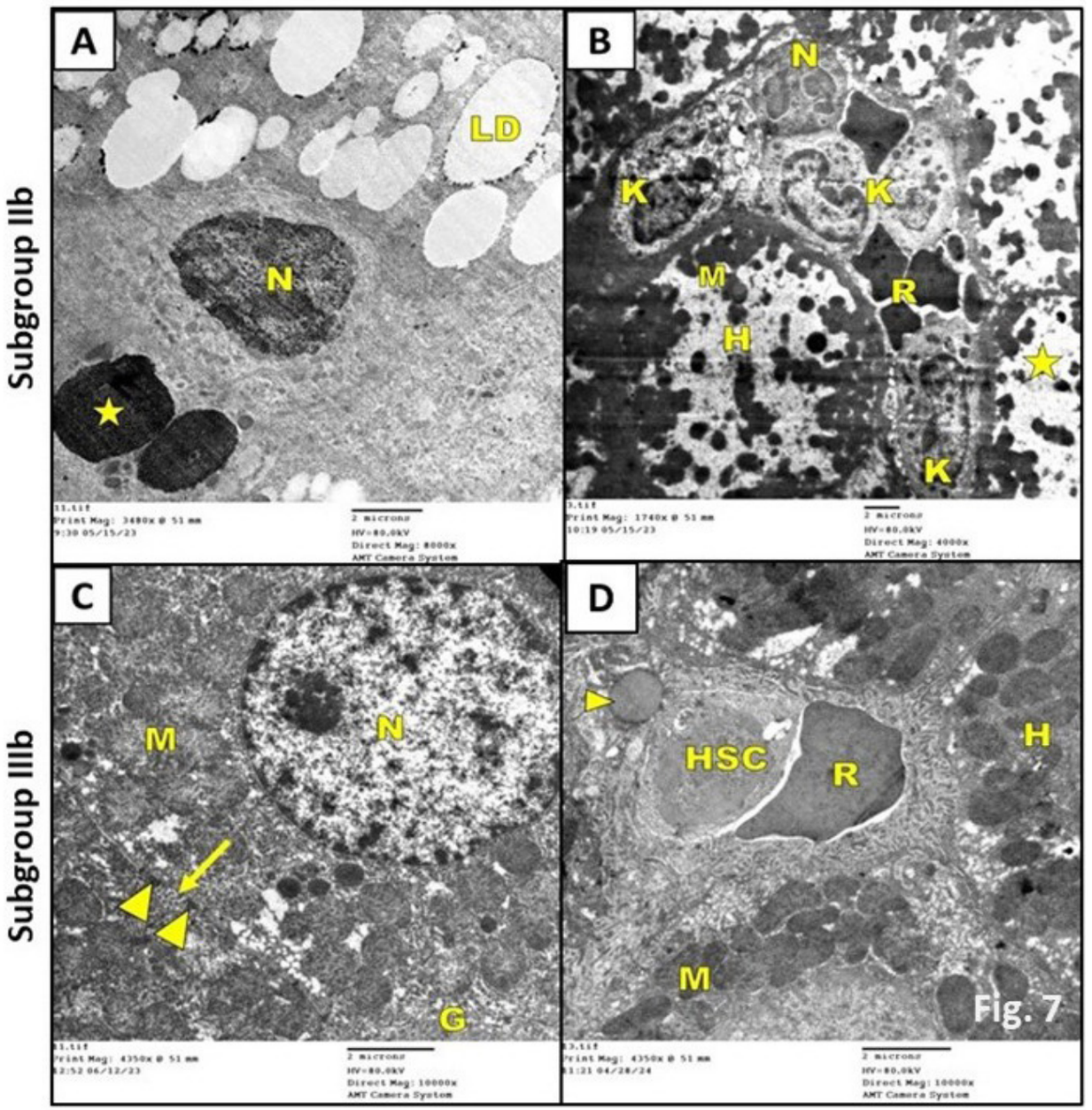

Fig. 7: transmission electron micrographs of different groups. [A] subgroup IIb: shows heterochromatic nucleus (N) with irregular nuclear membrane. Plenty of lipid droplets of variable size and shape with well-defined edges are scattered in the cytoplasm, most of them appear with low electron density (LD), while others appear with high electron density (the star). [B] subgroup IIb: shows blood sinusoids with multiple Kupffer cells (K) containing electron dense particles. Numerous RBCs (R) and a neutrophil cell (N) with the multi-segmented nucleus were also seen. The hepatocytes (H) show extensively rarified cytoplasm (the star) and electron dense mitochondria (m) with indistinct cristae. [C] subgroup IIIb: shows a nucleus (N) with a little amount of heterochromatin and regular nuclear membrane. Most of the mitochondria appear with well-defined membrane cristae (M). Glycogen granules are demonstrated (G). Notice the bile canaliculus (↑) with microvilli projecting into its the lumen and the nearby junctional complex (►). [D] subgroup IIIb: shows hepatocytes (H), the hepatic stellate cell (HSC) with a lipid droplet (►) in its cytoplasm in the perisinusoidal space. A red blood cell is seen (R) in the sinusoidal lumen. TEM, Fig.A x8000, Fig.B x4000, Fig.C x10000, Fig.D x10000

Table 1: displays the variations in the area % of collagen fibers in each group, expressed as mean ± standard deviation

	Group I	Subgroup IIa	Subgroup IIIa	Subgroup IIb	Subgroup IIIb
Area percentage of collagen fibers (%)	0.481±0.0974 (■ ♦)	5.236±1.2620 (*▲)	0.755±0.2135 (■)	7.042±1.841 (*●)	0.275 ± 0.0836 (♦)

* Significant variation from group I.
■ Significant variation from subgroup IIa.
▲ Significant variation from subgroup IIIa.
♦ Significant variation from subgroup IIb.
● Significant variation from subgroup IIIb.

Table 2: ALT and AST changes in various groups are displayed as mean ± standard deviation

	Group I	Subgroup IIa	Subgroup IIIa	Subgroup IIb	Subgroup IIIb
ALT (IU/L)	26.86 ±2.437 (■ ♦)	79.28 ±6.687 (*▲)	28.56 ±7.522 (■)	81.18 ±6.619 (*●)	27.16 ±7.249 (♦)
AST (IU/L)	24.56 ±5.933 (■ ♦)	90.1 ±15.536 (*▲)	24.64 ±7.360 (■)	92.08±14.990 (*●)	23.38 ±7.228 (♦)

* Significant variation from group I.
■ Significant variation from subgroup IIa.
▲ Significant variation from subgroup IIIa.
♦ Significant variation from subgroup IIb.
● Significant variation from subgroup IIIb.

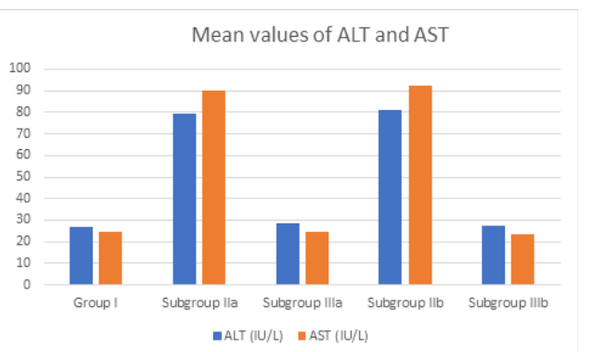

Histogram 2: The average ALT and AST measurements across the various groups

DISCUSSION

Although the last three decades have seen improvements in the outcomes for ALF patients, the mortality rate remains unacceptable, and more advancements in management are advised[18], so the current study demonstrated the impact of MSC derived exosomes on hepatic regeneration in adult male albino rats that have had acute liver damage caused by carbon tetrachloride.The effect of MSC-Exosomes as a new line of treatment had been investigated to improve the prognosis of the disease and reduce its mortality.

Since CCl4 is one of the most researched xenobiotics that cause hepatotoxicity in rats, it is used in the current study[19]. The hepatotoxicity mechanisms of CCl4 can be deduced from the generation of free radicals formed from CCl4, inflammatory cytokines, calcium homeostasis loss, lipid peroxidation, covalent binding to macromolecules, and hypomethylation of nucleic acids[20].

The intraperitoneal injection of a single dose of CCl4 has changed the liver's overall morphology in the present investigation. After two weeks, the livers of subgroup IIb displayed firm consistency, brittle texture, and pale light color in comparison with those of the control groups. This discoloration might be due to the congestion and the steatosis (fatty liver) caused by CCl4. The current findings were similar to previous studies relating such discoloration to hepatic tissue injury due to CCl4 administration[21]. The liver coloration appeared darker with the administration of a single dose of exosomes in the subgroup IIIb.

All subgroups treated with CCl4 (group II) showed variant degrees of centrilobular necrosis. Exosome-treated rats showed a considerable improvement in the pericentral and periportal hepatic cell lesions, collagen deposition, and mononuclear cellular infiltration compared to the CCl4-treated group.

In accordance with the current findings, it was mentioned that CCl4 in a rat model induced necrosis of hepatocytes and disorganization of sinusoids specially in the centrilobular zone. The cytochrome P450s that the centrilobular hepatocytes produce in large quantities metabolize several chemical hepatotoxins, such as carbon tetrachloride (CCl4), to produce extremely reactive free radicals that injure hepatocytes[22].

In the current investigation, light microscopic analysis of liver sections from rats treated with CCl4 (subgroup IIa)

revealed that some hepatocytes in the centrilobular zone appeared shrunken, deeply acidophilic, irregular, and with darkly stained nuclei, while the majority of hepatocytes appeared swollen with vacuolated cytoplasm (ballooned hepatocytes). Over time, these modifications became more noticeable and could be seen in more detail in subgroup IIb. These morphological alterations resemble those that Dutta *et al*.[23] have reported.

Regarding the hepatocytes' apparent vacuolations and ballooning, this could be explained by the low partial pressure of oxygen causing the creation of CHCl2 and CCl3 radicals from CCl4 metabolism. These radicals then disturb the metabolism of lipids, leading to fatty liver disease or steatosis. Although the high partial pressure of oxygen in the current study may have contributed to the dark, acidophilic hepatocytes with condensed nuclei, which change CCl4 metabolisms to produce the CCl3-OO radical and lipid peroxidation that moves the cells from steatosis to death[23].

Electron microscopic examination of the current study interpreted the presence of hepatocytes vacuolations. It revealed the presence of multiple fat droplets, which are more numerous in subgroup IIb than subgroup IIa, in the cytoplasm of the hepatocytes. Most of the lipid droplets seen with low electron density, while others were electron dense (saturated fat). The hepatocyte nuclei appeared shrunken irregular with increased heterochromatin which explain the pyknotic appearance in the Hematoxylin and Eosin sections. The pyknosis and chromatin condensation resulted from the necrosis induced by the CCl4 toxicity. Similarly, hepatocytes from CCl4-treated rats showed a considerable rise in immunological reactivity for the proapoptotic agent p53 in the cytoplasm in a recent study[24].

Some hepatic blood sinusoids of subgroup IIa were disorganized and obliterated that could be due to the ballooning of the hepatocytes. In subgroup IIb, the sinusoids appeared congested which was also obvious in the TEM sections of the current study. That sinusoidal congestion goes along with a previous study relating it to the toxic effect of CCl4[25].

In this study, compared to the control group, there appeared to be a greater quantity of bile ductules in the Haematoxylin and Eosin sections of the CCl4 treated group (Group II), particularly in subgroup IIb. One explanation could be that the liver cells were attempting to help with hepatic regeneration by transdifferentiating. During ductular reactions (DR), cholangiocytes, hepatocytes, or hepatic progenitor cells can be the source of active cells. In a similar vein, Omar *et al*.[26] reported that exposure to carbon tetrachloride (CCl4) in rats could cause proliferation of bile ducts. The ductular reaction was characterised by the development of reactive bile ducts caused by liver injury. In biliary disorders, bile duct hyperplasia was referred to as ductular response. Furthermore, a range of liver disease like nonalcoholic fatty liver may exhibit it[27].

The present study's CCl4-treated group showed little cellular infiltrations in the hematoxylin and eosin sections. This could be because CCl4 has an inflammatory effect. The presence of hepatocytic necrosis was verified by the cellular infiltrations. These results were also reported by Endig *et al*.[28], who noted that the innate immune system acts as the first line of defense and is activated far more quickly than adaptive immunity in cases of acute liver injury when the host has limited time to initiate an effective adaptive immune response[29]. This perspective is confirmed by the appearance of multiple Kupffer cells and neutrophils in the hepatic sinusoids detected by the transmission electron microscope of the current study.

Some areas of the hepatic lobules of subgroup IIb showed loss of the hepatic tissue and hemorrhage denoting the occurrence of necrosis which led to dropout and loss of hepatocytes. Such findings were similar to a retrospective study cohort showing massive or sub-massive necrosis in 48 livers taken after ALF patients' transplantation. They revealed areas with hepatocyte loss[30].

Regarding the appearance of the cells with spindle shaped nuclei between the hepatocytes of subgroup IIb of the current study, which were detected in H&E sections, these cells could probably be activated HSCs (myofibroblast like cells). The transmission electron microscopy of the current study observed that the hepatic stellate cells appeared with spindle shaped nuclei and were devoid of the cytoplasmic lipid droplets with nearby collagen fibrils. In the injured area, inflammatory and apoptotic parenchymal cells gather and release chemokines that stimulate HSCs. Activated HSCs become myofibroblast-like cells that release cytokines and form extracellular matrix (ECM) after losing their own lipid droplets[31].

In comparison to the control group (Group I), both subgroups of CCl4-treated rats had higher levels of collagen fiber deposition surrounding the portal area and the central vein, according to the Masson trichrome sections of the current study. Compared to subgroup IIa, collagen deposition was more noticeable in subgroup IIb. The morphometric analysis supported this observation by demonstrating a substantial increase in collagen area percentage in both subgroups (IIa and IIb) as compared to the control group. This was consistent with the findings of Chang *et al*.[32], who showed increased collagen deposition in a model of liver injury generated by CCl4.

Electron microscopic examination of all subgroups of rats treated by CCl4 revealed high rarefaction of the cytoplasm in both subgroups (IIa and IIb) in this study. In comparison to the control group, there appeared to be a decrease in both the quantity and size of mitochondria. The mitochondria appeared with high electron density coalescing with each other forming clumps in the cytoplasm. That might be due to the mitochondrial impairment caused by CCl4. Similarly, in a mouse model of CCl4-induced damage, Zhao *et al*.[33] found decreased mitochondrial mass and poor metabolism of the surviving mitochondria.

Glycogen granules and rough endoplasmic reticulum appeared to be declining as well. These electron

microscopic morphological changes detected in the present study were similar to those described by and Badr *et al*. who investigated how CCl4 affected rats' liver. They showed widespread cellular damage, pyknotic and shrunken nuclei with severe chromatin condensation, and hepatocyte cytoplasm lysis with an abnormally high number of lipid droplets and the absence of major cell organelles[34].

The bloodstream's release of liver enzymes (ALT and AST) from ruptured hepatocytes is a common sign of liver damage[35]. Accordingly, all subgroups treated with CCl4 (Group II) showed a substantial rise in blood liver function tests as compared to the control group. Carbon tetrachloride is metabolized in hepatocytes to the CCl3 radical, which is then changed into the highly reactive trichloromethylperoxy radical by the cytochrome P450 enzyme. Enzymes leak out as a result of the peroxidative membrane degradation brought on by the trichloromethylperoxy radical's covalent connection to the macromolecules[36].

The results of the current study showed that in adult male albino rats exposed to CCl4-induced acute hepatic failure, a single dosage of exosomes extracted from bone marrow-derived MSC might improve hepatocyte necrosis, decrease biochemical and histological hepatic injury, and increase survival of rats. These results are consistent with the comprehensive review of Shokravi *et al*.[37], which provided compelling evidence in favor of using MSC-Exosomes as a therapeutic intervention in cases of acute liver failure.

By light microscopy, more integrated hepatic tissue structure was observed in subgroup IIIa with a remarkable improvement of the hepatic architecture of subgroup IIIb which appeared nearly comparable to group I.

The majority of hepatocytes had pale acidophilic cytoplasm and spherical, vesicular nuclei. Most of hematoxylin and eosin sections lacked pyknotic nuclei. Reduced heterochromatin was also seen in the hepatocyte nuclei when the cells were examined with electron microscope. MSC-Exosomes may be able to slow down hepatocyte degeneration following acute liver injury, according to these results, which might be explained by increased expression of the antiapoptotic protein Bcl-2 and decreased expression of the pro-apoptotic proteins Bax and caspase-3[38].

The blood sinusoids were almost the same as those in the control group. The electron microscope used in this study confirmed that there was no sinusoidal congestion. However, in certain lobules of subgroup IIIa, there was still noticeable mild portal venous congestion with little periportal cellular infiltration. Neither periportal cellular infiltration nor portal vein congestion were seen in subgroup IIIb. These results corroborated those of Lin *et al*.[40] and Rostom *et al*.[39], who reported that MSC-Exosomes improved rat hepatic necrosis. MSC-derived exosomes have anti-inflammatory, cell proliferation-promoting, and M2 macrophage polarization-promoting qualities, which make them useful for treating liver damage[41].

There was no increase of the number of bile ductules in both subgroups IIIa and IIIb. The absence of the ductular reaction in the exosome treated group was denoting that the exosomes could improve the survival of the hepatocytes despite the injurious effect of CCl4.

Sections stained with Masson's trichrome revealed that subgroup IIIa had significantly more collagen fibers than subgroup IIIb, which had less collagen fibers that were almost identical to those of the control group. The morphometric study supported these findings that was going along with those of Ding *et al*.[42], who reported that MSC-produced exosome circDIDO1 overexpression inhibited HSC proliferation and reduced profibrotic markers. In the current investigation, the emergence of hepatic stellate cells in subgroup IIIa that were free of lipid droplets in the cytoplasm and had collagen fibrils close by suggested that these cells had been activated. HSCs in subgroup IIIb, however, kept their cytoplasmic lipid droplets without collagen fibrils, indicating that exosomes had an anti-fibrotic function. Chiabotto *et al*.,[43] on the other hand, observed an opposite outcome: Activated LX-2 hepatic stellate cells expressed more profibrotic markers when EVs generated from MSCs were compared to human hepatic stem cells. This might be as a result of COL1α1 being an EV generated from MSCs.

The hepatocytes in the current study did not have any fat droplets in the cytoplasm, according to electron microscopy analysis of the cells of both subgroups IIIa and IIIb. Subgroup IIIa had fewer mitochondria, which still had clearly defined cristae. The mitochondria in subgroup IIIb were similar to those in the control group.These results may corroborate a prior study's finding that exosomes prevent mitochondrial fission and stimulate mitochondrial fusion and biogenesis in order to preserve mitochondrial homeostasis[44].

Additionally, there appeared to be an increase in glycogen granules and rER.

Exosomes of MSCs upregulate TNF-activated NF-κB expression. In order to promote tissue regeneration, NF-κB activates local progenitor cells, promotes cell proliferation and differentiation, and mobilizes circulating stem cells[3]. Furthermore, hepatocyte growth factor (HGF) is widely distributed in exosomes generated from MSCs[45]. HGF is the most important mitogen for liver regeneration and repair after injury[46]. According to these viewpoints, the hepatocytes seen in the current investigation had reparative effects from supplied exosomes.

The liver damage caused by CCl4 had decreased after receiving exosome therapy. In all-treated rats of subgroup IIIa and IIIb, the hepatic enzyme levels significantly lowered to nearly normal, suggesting that exosomes can prevent enzyme leakage and minimize damage to cell membranes. These results go along with Abdel Hameed *et al*.[47] who reported that rats injured by CCl4 toxicity had their liver enzyme levels restored by MSC-exosomes.

CONCLUSION

Despite the regenerative power of the hepatic tissue, the liver couldn't regenerate and repair itself through two weeks after CCl4 induced toxicity. Consequently, the current study concluded that a single dose of exosomes produced from bone marrow mesenchymal stem cells may enhance hepatic regeneration following acute injury caused by CCl4. By exosomes injection, the hepatocytes were comparable to the control after two weeks histologically and biochemically.

CONFLICT OF INTERESTS

There are no conflicts of interest.

REFERENCES

1. Rai M, Paudel N, Sakhrie M, Gemmati D, Khan IA, Tisato V, Kanase A, Schulz A, Singh AV. Perspective on Quantitative Structure–Toxicity Relationship (QSTR) Models to Predict Hepatic Biotransformation of Xenobiotics. Livers. 2023; 3(3):448-462. https://doi.org/10.3390/livers3030032

2. Alexandrova R, Tsachev I, Kirov P, Abudalleh A, Hristov H, Zhivkova T, Dyakova L, Baymakova M. Hepatitis E Virus (HEV) Infection Among Immunocompromised Individuals: A Brief Narrative Review. Infect Drug Resist. 2024; 17:1021-1040. doi: 10.2147/IDR.S449221.

3. Zhang S., Hou Y., Yang J., Xie D., Jiang L., Hu H., Hu J., Luo C., & Zhang Q. Application of mesenchymal stem cell exosomes and their drug-loading systems in acute liver failure. Journal of cellular and molecular medicine. 2020, 24(13), 7082–7093. doi: 10.1111/jcmm.15290.

4. Wang C, Zhou H, Wu R, Guo Y, Gong L, Fu K, Ma C, Peng C, Li Y. Mesenchymal stem cell-derived exosomes and non-coding RNAs: Regulatory and therapeutic role in liver diseases. Biomed Pharmacother. 2023 Jan; 157:114040. https://doi.org/10.1016/j.biopha.2022.114040.

5. Moghadasi S, Elveny M, Rahman HS, Suksatan W, Jalil AT, Abdelbasset WK, Yumashev AV, Shariatzadeh S, Motavalli R, Behzad F, Marofi F, Hassanzadeh A, Pathak Y, Jarahian M. A paradigm shift in cell-free approach: the emerging role of MSCs-derived exosomes in regenerative medicine. J Transl Med. 2021 Jul 12;19(1):302. doi: 10.1186/s12967-021-02980-6.

6. Yin T, Liu Y, Ji W, Zhuang J, Chen X, Gong B, Chu J, Liang W, Gao J, Yin Y. Engineered mesenchymal stem cell-derived extracellular vesicles: A state-of-the-art multifunctional weapon against Alzheimer's disease. Theranostics. 2023 Feb 5;13(4):1264-1285. doi: 10.7150/thno.81860.

7. Maurya DK., Berghard A. & Bohm SA. Multivesicular body-like organelle mediates stimulus-regulated trafficking of olfactory ciliary transduction proteins. Nat Commun. 2022, 13, 6889. doi: 10.1038/s41467-022-34604-y.

8. Koh HB, Kim HJ, Kang SW, Yoo TH. Exosome-Based Drug Delivery: Translation from Bench to Clinic. Pharmaceutics. 2023 Jul 29;15(8):2042. doi: 10.3390/pharmaceutics15082042.

9. Magdy Beshbishy A, Alghamdi S, Onyiche TE, Zahoor M, Rivero-Perez N, Zaragoza-Bastida A, Ghorab MA, Meshaal AK, El-Esawi MA, Hetta HF, *et al*. Biogenesis, Biologic Function and Clinical Potential of Exosomes in Different Diseases. Applied Sciences. 2020; 10(13):4428. https://doi.org/10.3390/app10134428

10. Hassanzadeh A, Rahman HS, Markov A, Endjun JJ, Zekiy AO, Chartrand MS, Beheshtkhoo N, Kouhbanani MAJ, Marofi F, Nikoo M, Jarahian M. Mesenchymal stem/stromal cell-derived exosomes in regenerative medicine and cancer; overview of development, challenges, and opportunities. Stem Cell Res Ther. 2021 May 21;12(1):297. doi: 10.1186/s13287-021-02378-7.

11. Ghasempour E., Hesami S., Movahed E. *et al*. Mesenchymal stem cell-derived exosomes as a new therapeutic strategy in the brain tumors. Stem Cell Res Ther. 2022,13, 527. https://doi.org/10.1186/s13287-022-03212-4

12. Li X, Li C, Zhang L, Wu M, Cao K, Jiang F, Chen D, Li N, Li W. The significance of exosomes in the development and treatment of hepatocellular carcinoma. Mol Cancer. 2020 Jan 4;19(1):1. doi: 10.1186/s12943-019-1085-0.

13. Bala S., Calenda C.D., Catalano D., Babuta M., Kodys K., Nasser I.A., Vidal B. and Szabo G. Deficiency of miR-208a Exacerbates CCl4-Induced Acute Liver Injury in Mice by Activating Cell Death Pathways. Hepatol. Commun. 2020 Aug 19;4(10):1487-1501. doi: 10.1002/hep4.1540.

14. Anastasio A, Gergues M, Lebhar MS, Rameshwar P, Fernandez-Moure J. Isolation and characterization of mesenchymal stem cells in orthopaedics and the emergence of compact bone mesenchymal stem cells as a promising surgical adjunct. World J Stem Cells 2020 Nov 26;12(11):1341-1353. doi: 10.4252/wjsc.v12.i11.1341.

15. Coughlan C, Bruce KD, Burgy O, Boyd TD, Michel CR, Garcia-Perez JE, Adame V, Anton P, Bettcher BM, Chial HJ, Königshoff M, Hsieh EWY, Graner M, Potter H. Exosome Isolation by Ultracentrifugation and Precipitation and Techniques for Downstream Analyses. Curr Protoc Cell Biol. 2020 Sep;88(1):e110. doi: 10.1002/cpcb.110.

16. Corona ML, Hurbain I, Raposo G, van Niel G. Characterization of Extracellular Vesicles by Transmission Electron Microscopy and Immunolabeling Electron Microscopy. Methods Mol Biol. 2023; 2668:33-43. doi: 10.1007/978-1-0716-3203-1_4.

17. Suvarna S.K.; Layton C. and Bancroft J.D. (2019): Bancroft's Theory and Practice of Histological Techniques. eighth edition. Elsevier; 126-138, 153-175 and 434-475. ISBN 978-0-7020-6887-4 doi: https://doi.org/10.1016/C2015-0-00143-5

18. Aziz R, Price J, Agarwal B. Management of acute liver failure in intensive care. BJA Educ. 2021 Mar;21(3):110-116. https://doi.org/10.1016/j.bjae.2020.11.006

19. Cosgun B., Erdemli M., Gul M., Gul S., Bag H., Erdemli Z. and Altinoz E. Crocin (active constituent of saffron) improves CCl4-induced liver damage by modulating oxidative stress in rats. Turkish Journal of Biochemistry. 2019, Vol. 44 (Issue 3), pp. 370-378. https://doi.org/10.1515/tjb-2017-0173

20. Al Amin ASM, Menezes RG. Carbon Tetrachloride Toxicity. [Updated 2023 Sep 4]. In: StatPearls [Internet]. Treasure Island (FL): StatPearls Publishing; 2023 Jan-. Available from: https://www.ncbi.nlm.nih.gov/books/NBK562180/

21. Ko IG, Jin JJ, Hwang L, Kim SH, Kim CJ, Han JH, Lee S, Kim HI, Shin HP, Jeon JW. Polydeoxyribonucleotide Exerts Protective Effect Against CCl4-Induced Acute Liver Injury Through Inactivation of NF-κB/MAPK Signaling Pathway in Mice. Int J Mol Sci. 2020 Oct 24;21(21):7894. doi: 10.3390/ijms21217894.

22. Hora S, Wuestefeld T. Liver Injury and Regeneration: Current Understanding, New Approaches, and Future Perspectives. Cells. 2023; 12(17):2129. doi: 10.3390/cells12172129.

23. Dutta S, Chakraborty AK, Dey P, Kar P, Guha P, Sen S, Kumar A, Sen A, Chaudhuri TK. Amelioration of CCl4 induced liver injury in Swiss albino mice by antioxidant rich leaf extract of Croton bonplandianus Baill. PLoS One. 2018 Apr 30;13(4): e0196411. doi: 10.1371/journal.pone.0196411.

24. Abdel Fattah AA, Abdul-Hamid M, Almanaa TN, Alhaber LA, Abdel-Kawi SH, Abdel Rahman FES, Ahmed OM. Ameliorative effects of allogeneic and xenogenic bone marrow-derived mesechymal stem cells on carbon tetrachloride-induced rat liver injury and cirrhosis via modulation of oxidative stress, apoptosis, inflammation, and Nrf2 expression. Am J Transl Res. 2023 Nov 15;15(11):6381-6403. www.ajtr.org /ISSN:1943-8141/AJTR0152930

25. Aithal AP, Bairy LK, Seetharam RN, Kumar N. Hepatoprotective effect of bone marrow-derived mesenchymal stromal cells in CCl4-induced liver cirrhosis. 3 Biotech. 2021 Feb;11(2):107. doi: 10.1007/s13205-021-02640-y. Epub 2021 Jan 31.

26. Omar W., Zohdy N., Radi S., Elsheikh M., Abdel-Moneim R. Therapeutic Potential of Integrated Berberine Oleate Loaded Liposomes Versus Free Berberine in Carbon Tetrachloride Induced Liver Fibrosis in Rats: A Histological and Immunohistochemical Study. Egyptian Journal of Histology. 2022; 45(3): 875-893. doi: 10.21608/ejh.2021.80040.1502

27. Sato K, Marzioni M, Meng F, Francis H, Glaser S, Alpini G. Ductular Reaction in Liver Diseases: Pathological Mechanisms and Translational Significances. Hepatology. 2019 Jan;69(1):420-430. doi: 10.1002/hep.30878]. Hepatology. 2019;69(1):420-430. doi:10.1002/hep.30150

28. Endig J, Unrau L, Sprezyna P, Rading S, Karsak M, Goltz D, Heukamp LC, Tiegs G, Diehl L. Acute Liver Injury after CCl4 Administration is Independent of Smad7 Expression in Myeloid Cells. Int J Mol Sci. 2019 Nov 6;20(22):5528. doi:10.3390/ijms20225528

29. Khanam A, Kottilil S. Abnormal Innate Immunity in Acute-on-Chronic Liver Failure: Immunotargets for Therapeutics. Front Immunol. 2020 Oct 8; 11:2013. doi:10.3389/fimmu.2020.02013

30. Li J, Zhao YR, Tian Z. Roles of hepatic stellate cells in acute liver failure: From the perspective of inflammation and fibrosis. World J Hepatol. 2019 May 27;11(5):412-420. doi: 10.4254/wjh.v11.i5.412.

31. Hall A, Cotoi C, Luong TV *et al*. Collagen and elastic fibres in acute and chronic liver injury. Sci Rep. 2021, 11, 14569. https://doi.org/10.1038/s41598-021-93566-1

32. Chang SN, Kim SH, Dey DK, Park SM, Nasif O, Bajpai VK, Kang SC, Lee J, Park JG. 5-O-Demethylnobiletin Alleviates CCl4-Induced Acute Liver Injury by Equilibrating ROS-Mediated Apoptosis and Autophagy Induction. Int J Mol Sci. 2021 Jan 22;22(3):1083. doi: 10.3390/ijms22031083.

33. Zhao Z, Hou Y, Zhou W, Keerthiga R, Fu A. Mitochondrial transplantation therapy inhibit carbon tetrachloride-induced liver injury through scavenging free radicals and protecting hepatocytes. Bioeng Transl Med. 2020 Dec 30;6(2):e10209. doi:10.1002/btm2.10209

34. Badr G, Sayed EA, Waly H, Hassan KA, Mahmoud MH, Selamoglu Z. The Therapeutic Mechanisms of Propolis Against CCl4 -Mediated Liver Injury by Mediating Apoptosis of Activated Hepatic Stellate Cells and Improving the Hepatic Architecture through PI3K/AKT/mTOR, TGF-β/Smad2, Bcl2/BAX/P53 and iNOS Signaling Pathways. Cell Physiol Biochem. 2019;53(2):301-322. doi:10.33594/000000140

35. Shrestha R. L.; Adhikari A. Anti-leshmanial constituents from Corydalis govaniana Wall. European J. Biotechnol. Biosci. 2017, 5, 47−48. https://www.biosciencejournals.com/assets/archives/2017/vol5issue5/5-5-16-765.pdf

36. Jahan A, Shams S, Ali S, Samrana S, Ali A, Adhikari A, Sajid M, Ali A, Ali H. Govaniadine Ameliorates Oxidative Stress, Inflammation, and Kupffer Cell Activation in Carbon Tetrachloride-Induced Hepatotoxicity in Rats. ACS Omega. 2021 Jan 21;6(4):2462-2472. doi: 10.1021/acsomega.0c02261

37. Shokravi S., Borisov V., Zaman B.A. *et al*. Mesenchymal stromal cells (MSCs) and their exosome in acute liver failure (ALF): a comprehensive review. Stem Cell Res Ther. 2022, 13, 192 https://doi.org/10.1186/s13287-022-02825-z

38. Zhao S, Liu Y, Pu Z. Bone marrow mesenchymal stem cell-derived exosomes attenuate D-GaIN/LPS-induced hepatocyte apoptosis by activating autophagy in *vitro*. Drug Des Devel Ther. 2019; 13:2887-2897. doi:10.2147/DDDT.S220190

39. Rostom DM, Attia N, Khalifa HM, Abou Nazel MW, El Sabaawy EA. The Therapeutic Potential of Extracellular Vesicles Versus Mesenchymal Stem Cells in Liver Damage. Tissue Eng Regen Med. 2020;17(4):537-552.doi:10.1007/s13770-020-00267-3

40. Lin F., Chen W., Zhou J. *et al*. Mesenchymal stem cells protect against ferroptosis via exosome-mediated stabilization of SLC7A11 in acute liver injury. Cell Death Dis. 2022, 13, 271. https://doi.org/10.1038/s41419-022-04708-w

41. Arabpour M., Saghazadeh A., Rezaei N. Anti-inflammatory and M2 macrophage polarization-promoting effect of mesenchymal stem cell-derived exosomes. Int. Immunopharmacol. 2021;97:107823. doi:10.1016/j.intimp.2021.107823

42. Ding Y, Luo Q, Que H, Wang N, Gong P, Gu J. Mesenchymal Stem Cell-Derived Exosomes: A Promising Therapeutic Agent for the Treatment of Liver Diseases. Int J Mol Sci. 2022 Sep 19;23(18):10972. doi:10.3390/ijms231810972

43. Chiabotto G., Ceccotti E., Tapparo M., Camussi G., Bruno S. Human Liver Stem Cell-Derived Extracellular Vesicles Target Hepatic Stellate Cells and Attenuate Their Pro-Fibrotic Phenotype. Front. Cell Dev. Biol. 2021; 9:777462. doi:10.3389/fcell.2021.777462

44. Zhang Q, Piao C, Ma H, *et al*. Exosomes from adipose-derived mesenchymal stem cells alleviate liver ischaemia reperfusion injury subsequent to hepatectomy in rats by regulating mitochondrial dynamics and biogenesis. J Cell Mol Med. 2021; 25: 10152–10163. doi:10.1111/jcmm.16952

45. Yu L, Xue J, Wu Y, Zhou H. Therapeutic effect of exosomes derived from hepatocyte-growth-factor-overexpressing adipose mesenchymal stem cells on liver injury. Folia Histochem Cytobiol. 2023;61(3):160-171. doi:10.5603/fhc.95291

46. Zhao Y, Ye W, Wang YD, Chen WD. HGF/c-Met: A Key Promoter in Liver Regeneration. Front Pharmacol. 2022 Mar 17; 13:808855. doi:10.3389/fphar.2022.808855

47. Abdel Hameed AM, Mortada SA, Morcos MA, Mahmoud AH. A Comparative Histological Study On The Therapeutic Effect of Mesenchymal Stem Cells Versus Exosomes on CCL4 Induced Liver Injury in Adult Male Albino Rats. Egyptian Journal of Histology 2024 June; 47 (2): 739-757 doi: 10.21608/ejh.2023.206683.1884

الملخص العربى

دورالإكسوزومات من الخلايا الجذعية الوسيطة في تجديد النسيج الكبدى بعد نلف الكبد الحاد بواسطة رابع كلوريد الكربون في ذكور الجرذان البيضاء البالغة. (دراسة هستولوجية)

غادة لطفي، نيفرت فريد عبد السلام، سهام كامل أبوناصف، سمر ف عزت

قسم الهستولوجي، كلية الطب، جامعة عين شمس، مصر

الخلفية: يعد الفشل الكبدى الحاد أحد الحالات الطارئة. تستخدم الخلايا الجذعية الوسيطة المشتقة من نخاع العظام على نطاق واسع في الطب التجديدي.

الهدف : توضيح تأثير الإكسوزومات المشتقة من الخلايا الجذعية الوسيطة على تجديد النسيج الكبدى في حالة الفشل الكبدى الحاد المستحث بواسطة رابع كلوريد الكربون في ذكور الجرذان البيضاء البالغة.

المواد والطرق: تم تقسيم ٥٥ جرذاً بالغاً إلى ثلاث مجموعات: المجموعة الأولى (التحكم)، المجموعة الثانية (تم حقنها من خلال الغشاء البريتونى بجرعة واحدة من رابع كلوريد الكربون) والمجموعة الثالثة (تم حقنها من خلال وريد الذيل بمقدار ٥٠ ميكروجرام من الإكسوزومات المشتقة من الخلايا الجذعية الوسيطة في ١٠٠ ميكرولتر من محلول الفوسفات الملحي). تم التضحية بالفئران بعد ٧ و١٤ يومًا. تم إجراء الفحص النسيجي لأنسجة الكبد مع التحليل الكيميائي الحيوي لإنزيمات الكبد.

النتائج: كشفت المجموعة الثانية عن تغير في بنية الكبد مع ظهور بؤر من التسلل الخلوي و احتقان وتوسع الأوردة البابية والمركزية. ظهر انسداد وعدم انتظام فى الجيوب الدموية للنسيج الكبدى. ظهرت معظم خلايا الكبد مع سيتوبلازم داكن اللون ونواة مكثفة، في حين ظهرت خلايا أخرى مع نواة صغيره داكنه وسيتوبلازم مفرغ. وقد شوهدت زيادة كبيرة في ألياف الكولاجين. من خلال فحص الميكروسكوب الالكترونى النافذ ، ظهرت خلايا الكبد بنوى غير متجانسة وغير منتظمة وسيتوبلازم مفرغ مع الكثير من قطرات الدهون. انخفضت أعداد الميتوكوندريا وأحجامها. كانت الخلايا النجمية الكبدية خالية من قطرات الدهون. احتوت الجيوب الدموية علي خلايا كوبفر متعددة. كانت هناك زيادة كبيرة في مستويات انزيمات الكبد بالدم. كشفت المجموعة المعالجة بالإكسوسومات عن تحسن في التغيرات النسيجية والكيميائية الحيوية المذكورة سابقًا.

الاستنتاج: فشل تجديد الكبد وإصلاحه خلال أسبوعين بعد التسمم المستحث بواسطة رابع كلوريد الكربون. أدت جرعة واحدة من الإكسوزومات المشتقة من الخلايا الجذعية الوسيطة للنخاع العظمي إلى تحسين عملية تجديد الكبد بعد الإصابة الحادة الناجمة عن رابع كلوريد الكربون.